Research Square

Preprints are preliminary reports that have not undergone peer review.
They should not be considered conclusive, used to inform clinical practice,
or referenced by the media as validated information.

A basin-wide Arctic ice shelf reverses deep ocean circulation

Pengyang Song

Pengyang.Song@awi.de

Alfred Wegener Institute, Helmholtz Centre for Polar and Marine Research https://orcid.org/0000-0003-1791-9454

Gregor Knorr

Alfred Wegener Institute, Helmholtz Centre for Polar and Marine Research https://orcid.org/0000-0002-8317-5046

Gerrit Lohmann

Alfred Wegener Institute https://orcid.org/0000-0003-2089-733X

Article

Keywords:

Posted Date: February 25th, 2026

DOI: https://doi.org/10.21203/rs.3.rs-8848433/v1

License: This work is licensed under a Creative Commons Attribution 4.0 International License.
Read Full License

Additional Declarations: There is **NO** Competing Interest.

A basin-wide Arctic ice shelf reverses deep ocean circulation

Pengyang Song[1*], Gregor Knorr[1] and Gerrit Lohmann[1,2]

[1*]Alfred Wegener Institute, Helmholtz Centre for Polar and Marine Research (AWI), Klussmannstr. 3, 27570, Bremerhaven, Germany.
[2]MARUM–Centre for Marine Environmental Sciences, University of Bremen, Leobener Str. 8, 28359, Bremen, Germany.

*Corresponding author(s). E-mail(s): pengyang.song@awi.de;

Abstract

Geological evidence suggests that a kilometre-thick ice shelf may have covered the Arctic Mediterranean (AM)—comprising the Arctic Ocean and Nordic Seas—during one or more glacial periods. However, the broader climatic and oceanographic implications of such a scenario remain poorly understood. Here, for the first time, we use a comprehensive Earth system model that explicitly resolves sub-ice-shelf circulation to explore the consequences of a fully glaciated AM. Our simulations reveal a fundamentally altered glacial ocean state: the expansive ice shelf reverses the overturning circulation within the AM—from dense-water sinking to deep-water upwelling—and suppresses North Atlantic Deep Water formation through sustained meltwater discharge from the AM. The persistent connection between the AM and the North Atlantic is maintained by a continuous Atlantic inflow through the Faroe–Shetland Channel, which prevents the AM from freshening. Hence, our results do not support the previously proposed hypothesis that freshwater could have accumulated beneath such a gigantic ice shelf, underscoring the critical role of ice shelf–ocean interactions in shaping glacial deep-water circulation.

1 Introduction

During the last glacial cycle, massive ice sheets expanded across the high northern latitudes, profoundly transforming the Arctic environment. Marine geological records indicate that the Arctic Ocean and adjacent Nordic Seas—collectively termed the Arctic Mediterranean (AM)—may have been covered by an extensive, kilometre-thick floating ice shelf resembling present-day West Antarctica (Mercer 1970; Broecker 1975; Hughes et al. 1977). Evidence for such a configuration derives from bathymetric mapping, sub-bottom profiling, seismic reflection data, and sediment cores, which document ice-shelf grounding or iceberg scouring across multiple Arctic bathymetric highs, including the Beaufort Margin, Chukchi Borderland, Siberian Shelf edge, Lomonosov Ridge, Yermak Plateau, and Jan Mayen Ridge (Engels et al. 2008; Jakobsson et al. 2008; Niessen et al. 2013; Polyak et al. 2001, 2007; Dowdeswell et al. 2010; Dowdeswell and Ottesen 2024). Most records date to Marine Isotope Stages 4 or 6, with the deepest grounding evidence reaching approximately 1000 m at the Lomonosov Ridge. Together, these observations have motivated the hypothesis of a basin-wide, kilometre-thick Arctic ice shelf during past glacial periods (Jakobsson et al. 2010, 2016; Geibert et al. 2021), although this interpretation remains debated (Stein et al. 2017; Knies et al. 2025). Such an ice shelf would have fundamentally altered ocean–atmosphere exchange, sea-ice formation, and deep-water circulation, yet its climatic consequences remain poorly constrained because coupled climate models have until recently lacked the capability to resolve ocean circulation beneath thick ice shelves.

Despite numerous efforts to reproduce glacial climates (Kageyama et al. 2021), this hypothesised "hyper-glacial" Arctic Mediterranean (AM) state has rarely been explored using numerical models. Previous studies have typically focused on individual components, such as the atmosphere or ice sheets alone (Colleoni et al. 2011; Nilsson et al. 2017; Gasson et al. 2018), and have therefore been unable to address the coupled dynamics of ocean circulation beneath a basin-wide ice shelf. This limitation

has become particularly salient in light of a recent debate over whether a freshwater reservoir could have existed beneath a kilometre-thick ice shelf spanning the AM (Geibert et al. 2021; Spielhagen et al. 2022; Hillaire-Marcel et al. 2022), highlighting the need to examine the ice-shelf hypothesis from an integrated climate-system perspective that explicitly resolves sub–ice-shelf ocean dynamics. Here, we address this gap using a comprehensive Earth system model that fully couples the ocean, atmosphere, and land surface, and includes a prescribed ice sheet–ice shelf component with an explicit representation of sub–ice-shelf circulation (Song et al. 2025). We show that a kilometre-thick, basin-wide ice shelf fundamentally reorganises the glacial climate state (Fig. 1): overturning circulation within the AM is reversed, North Atlantic Deep Water formation is suppressed, and the glacial Atlantic Meridional Overturning Circulation collapses. Crucially, despite sustained meltwater input, the AM does not transition to a freshwater basin, because saline Atlantic inflow persists through the Faroe–Shetland Channel, preventing freshwater isolation.

2 Results

The AM ice shelf primarily affects the ocean through two mechanisms: basal meltwater input and reorganisation of overturning and gateway exchange. These changes cascade into gyre structure and climate. We take the Last Glacial Maximum (LGM) as a representative glacial period and conduct two 800-year simulations initialised from a spun-up LGM climatology: CTRL serves as the control simulation using the LGM (21 ka) ice-sheet configuration (Tarasov et al. 2012), while ICE includes the hypothesised ice shelf. We implement the most extensive hypothesised configuration—an ice shelf covering the entire AM and extending slightly southward beyond the Greenland–Scotland Ridge (GSR)—hereinafter referred to as the AM ice shelf (Fig. A1b). The AM ice shelf is uniformly 1000 m thick across the Arctic Ocean and linearly thins towards its southern calving front at the GSR. From year 500 of ICE, we branch off

a third 300-year simulation, ICEfw, which incorporates a 0.1-Sv subglacial freshwater discharge along the Arctic grounding line at 1000 m, to explore the influence of subglacial hydrology (e.g. discharge from subglacial lakes). With these simulations, we show that the ocean and climate system can be largely influenced by the AM ice shelf in the following respects.

Firstly, the AM ice shelf alters freshwater input into the ocean (Fig. 2). In CTRL, the net surface freshwater flux to the AM basin is 0.07 Sv, comprising sea-ice and atmospheric processes (−0.06 Sv) and river runoff (0.13 Sv). By contrast, in ICE, the freshwater flux is exclusively generated by ice-shelf basal melt, as the ice shelf inhibits sea-ice formation and atmospheric exchange. The total basal melt rate of the AM ice shelf is 0.35 Sv, including 0.13 Sv south of the GSR, 0.19 Sv in the Nordic Seas, and 0.03 Sv in the Arctic Ocean. These basal melt rates in ICE demonstrate spatial inhomogeneity. Model results show elevated melt along the eastern boundary of the cavity ocean and beneath sloping ice-shelf bases (Fig. 2b). Furthermore, subglacial freshwater discharge increases basal melt in the Arctic Ocean (0.17 Sv, including 0.1 Sv discharge) and the Nordic Seas (0.22 Sv), while slightly decreasing it south of the GSR (0.12 Sv). Note that the model produces striped and noisy melt-rate patterns due to pressure gradient calculation deviations introduced by partial cells in cavities—an unresolved issue in z-coordinate simulations (e.g. Mathiot et al. 2017).

Ice shelf–ocean interaction substantially modifies the hydrographic structure in the AM (Figs. 3 and 4). With a thick ice shelf capping the upper ocean, ICE shows that basal melting strongly freshens the cavity ocean at the ice shelf–ocean interface, and this freshening signal gradually penetrates deeper (Fig. 3c,d). A much weaker freshening trend in CTRL supports that the signal in ICE is not caused by model drift. Simultaneously, latent heat from basal melting cools the surface cavity ocean, while the absence of wind-driven mixing and brine rejection results in a warmer deep ocean (Fig. 4c,d). Similarly, previous research proposed that a more extensive ice-covered

AM during past glacial periods led to a warmer-than-present, poorly ventilated and anoxic deep AM (Cronin et al. 2012; Thornalley et al. 2015; Jang et al. 2023), though a scenario with basin-wide ice shelf was not discussed. In ICEfw, subglacial freshwater discharge intensifies surface freshening in the Arctic Ocean beneath the ice shelf, where salinity decreases to around 30 psu by the end of the simulation. This brackish layer further freshens the deeper cavity ocean.

Complete glaciation of the AM fundamentally reverses vertical overturning circulation in the Nordic Seas and disrupts AM–North Atlantic water exchange (Fig. 1). Under atmospheric forcing, CTRL exhibits atmospheric cooling, wind-driven mixing, and deep-water formation in the Nordic Seas. In contrast, ICE exhibits upwelling and freshening of deep waters due to basal melt. As a result, the dense water flow over the GSR (i.e. Denmark Strait overflow) in CTRL disappears in ICE, replaced by outflowing meltwater. The ice shelf imposes a solid upper boundary, eliminating surface currents and partially obstructing upper-level transport through the GSR channels. ICE shows that Atlantic inflow through the Faroe–Shetland Channel shifts to lower depths, through the Iceland–Faroe Branch is replaced by meltwater outflow, and through the Denmark Strait, polar surface outflow is eliminated. Compared with ICE, ICEfw enhances overturning by strength and spatial extent, boosting AM–North Atlantic exchange. Beneath the ice shelf, Arctic circulation appears stagnant in ICE but is invigorated by subglacial discharge in ICEfw. Both simulations exhibit a secondary circulation beneath the main cell, stimulated by mixing over ridges in the Nordic Seas.

The kilometre-thick AM ice shelf amplifies topographic effects on horizontal gyres (Fig. 1). The barotropic streamfunction in ICE displays strengthened horizontal gyres confined within the Norwegian, Lofoten, and Greenland basins, which are separated by the Jan Mayen Fracture Zone and Mohn Ridge (Fig. A2b). Since large-scale geostrophic flows generally follow f/H contours (f being planetary vorticity and H

water depth), reductions in H intensify topographic constraints (Fig. A3), especially when water depth is reduced by almost 1000 m. Notably, an anticyclonic gyre develops west of the Yermak Plateau in ICE—counter to the dominant cyclonic gyres in the region. This gyre is weak in ICE but expands substantially in ICEfw, shifting its southern boundary to Mohn Ridge, between Lofoten and Greenland basins. Thus, ICEfw exhibits a double-gyre system in the Nordic Seas beneath the ice shelf: a southern cyclonic gyre featuring Atlantic inflow along its eastern boundary and meltwater outflow along its western boundary, and a northern anticyclonic gyre with meltwater outflow along its eastern boundary and deeper inflow along its western boundary (Fig. A2c).

Lastly, the AM ice shelf markedly shifts the climate state. With the suppression of dense-water formation and addition of meltwater in the AM, both ICE and ICEfw exhibit a complete shutdown of NADW formation (Fig. 5). This pattern mimics the "off" mode of Atlantic Meridional Overturning Circulation (AMOC) previously reported (e.g. Rahmstorf 2002; Böhm et al. 2015). The NADW shutdown reduces meridional heat transport, resulting in a colder North Atlantic climate and a warmer southern pole relative to CTRL (Fig. A4b,c), which demonstrates a thermal bipolar seesaw (Knutti et al. 2004). A cooler Arctic atmosphere is also evident in ICE and ICEfw, primarily due to inhibited atmosphere–ocean heat flux, and secondarily due to increased mean albedo. It has been suggested that Arctic cooling also results from considering surface elevation of ice shelves (Colleoni et al. 2010), though this effect is not represented in our study as we do not apply changes in surface elevation.

3 Discussion

Previous studies have investigated overturning circulation in ice-shelf cavities in the southern hemisphere (e.g. Hellmer and Olbers 1989; Grosfeld et al. 1997; Losch 2008), and it is widely agreed that the driver of overturning originates from melting along a

sloping ice-shelf base. This process freshens and cools seawater, creating a density and pressure gradient along the base—commonly referred to as the "ice pump" mechanism (Lewis and Perkin 1986). Assuming a deeper ice-shelf base towards the pole, one can infer that the Coriolis force and the pressure gradient together drive meltwater westward (applicable in both hemispheres). Since ice-shelf meltwater is transported westward, it can only exit the cavity upon reaching the western boundary, forming a strong upwelling along the ice shelf's western boundary. During this upwelling, the meltwater may reach below the ambient pressure melting point, resulting in refreezing at the western calving front. Meanwhile, the inflow of warm water from the open ocean acts as a compensating flow. ICE verifies this mechanism by demonstrating a cyclonic gyre dominating the Nordic Seas—with Atlantic inflow through the Faroe–Shetland Channel and meltwater outflow via the Denmark Strait—alongside slight refreezing of the ice shelf in southwestern AM. ICE also highlights the role of pressure gradients in driving sub-ice flows by showing a stagnant Arctic Ocean beneath a flat ice-shelf base.

In addition, geostrophic balance implies that f/H contours predominantly constrain circulation beneath the ice shelf, effectively steering flow along bathymetric ridges. Barotropic streamfunctions largely follow isobaths, as planetary vorticity (f) changes little at high latitudes. In both ICE and ICEfw, gyres are more strongly confined by ridges due to reduced water thickness and thereby the amplified f/H effect. Notably, ICEfw reveals an anticyclonic gyre in the north, initiated by subglacial freshwater discharge and increased basal melt in the Arctic. This gyre is characterised by freshwater flowing southward along the eastern boundary and a compensating deep current flowing northward into the Arctic basin. Absent from previous studies, we speculate that this feature is primarily guided by the Spitsbergen and Molloy Fracture Zones at the Fram Strait through the f/H constraint. The meltwater then transits westward along the Mohn Ridge, converging with meltwater from the southern

cyclonic gyre. Nevertheless, it should be noted that the assumed subglacial freshwater discharge (0.1 Sv) is relatively large—more than twice the present Antarctic basal melt rate (1265 Gt yr^{-1} or 0.04 Sv) (Adusumilli et al. 2020).

Achieving a fully freshwater basin appears implausible, though the AM ice shelf significantly freshens the basin underneath. Time series of basin-averaged AM salinity show rapid freshening in the initial 300 model years, after which the freshening rate steadily declines (Fig. 6a). A fully glaciated AM system adheres to a basic salt conservation principle: the tendency of salinity, virtual surface salt flux within the cavity, and salt advection across the AM southern boundary must be balanced. Applying this framework, we find that although 0.22 Sv of freshwater is introduced via basal melt, simultaneous net salt import through the GSR channels yields only a modest salinity decline (Fig. 6b–d). This net salt import arises from the residual between salty Atlantic inflow and fresher meltwater-dominated outflow. Subglacial freshwater discharge seems to be an efficient way to freshen the basin, but note that stronger basal melt and meltwater outflow are meanwhile accompanied by stronger compensating Atlantic inflow (ICEfw), which prevents the AM basin from reaching a freshwater state—even over longer simulations. Moreover, the f/H barrier from the ice-shelf front and bathymetric ridges could fail to block inflow along the lateral boundaries (Stern et al. 2014).

Our model's capability and configuration prevent us from fully unraveling the ice-shelf hypothesis or definitively rejecting the freshwater hypothesis. As our model applies a passive ice-sheet–ice-shelf system as a boundary condition, the establishment and collapse of such a basin-wide ice shelf within a dynamic Earth system remain unresolved. Additionally, our modelling study remains constrained within a geostrophic regime, though it benefits from relatively high polar and coastal resolution (20 km) due to the unstructured ocean mesh. Therefore, the key factor in forming a freshwater-filled AM basin—dynamical isolation from the Atlantic—can only be excluded within

the geostrophic regime, as our results show vigorous saline inflow through the Faroe–Shetland Channel. However, when the channel scale drops below the Rossby radius of deformation horizontally, or water thickness becomes sufficiently small vertically, circulation transitions from rotationally to hydrologically controlled, enabling the formation of a freshwater reservoir (Jakobsson et al. 2007; Stärz et al. 2017; Nilsson et al. 2023). Nevertheless, it is important to emphasise that, to date, no geological evidence has been found for an almost complete cut-off of the AM–Atlantic connection during the Pleistocene.

Our work demonstrates a prototype of ocean circulation beneath the AM ice shelf. However, it should be noted that our study employs an idealised ice-shelf geometry, and the reconstructed LGM ocean bathymetry contains uncertainties. Indeed, the dating of deep ice-shelf grounding evidence remains under debate, and our study adopts the LGM as a representative glacial period. We acknowledge that bathymetry and ice-shelf geometry may have been more complex during earlier glacial periods, potentially altering ocean circulation. Nonetheless, the fundamental ocean dynamics should remain consistent.

Finally, since our results show that a sub-ice cavity ocean can be overturned by a deep-ocean buoyancy source, we highlight several related processes. Deep-ocean mixing plays a crucial role in circulating deep water under the AM ice shelf, as overturning streamfunctions in ICE and ICEfw indicate vigorous mixing in the deep Nordic Seas. Therefore, ocean mixing rate, which is largely affected by current shear and topography roughness, could be a key parameter in controlling sub-ice circulation. Tidal motion is another important source of mixing. However, the presence of a thick ice shelf likely damps tidal energy and suppresses tidal mixing, although a reduced Arctic basin size during glacial periods inherently amplifies tidal activity (Griffiths and Peltier 2008). Furthermore, inspired by the enhanced cavity overturning due to freshwater discharge at a 1000 m grounding line, other external forcings that provide deep-ocean

buoyancy—such as geothermal heating, estimated at $40\,\mathrm{mW\,m^{-2}}$ to $60\,\mathrm{mW\,m^{-2}}$ in the modern Arctic (Timmermans et al. 2003)—could also be significant.

4 Concluding remarks

The hypothesis of a kilometre-thick ice shelf spanning the Arctic Mediterranean has long captured scientific interest, yet its consequences for ocean circulation have remained untested in a fully coupled climate model. Despite some caveats regarding model configuration, our study provides a novel benchmark: for the first time, a fully glaciated AM is explored within a comprehensive ESM, offering a physically consistent and dynamically rich reconstruction of an alternative ocean and climate state. Our results show that an extreme AM-wide ice shelf fundamentally reorganises AM hydrography, gyre structure, and overturning strength, with consequences that include a shutdown of the glacial AMOC. Nevertheless, even under kilometre-thick ice and substantial freshwater input, a full transition to a freshwater state does not emerge under the dynamically connected conditions explored here. Instead, geostrophically constrained gateways—particularly the wide Faroe–Shetland Channel—maintain the inflow of saline Atlantic waters, preventing freshwater isolation.

Moreover, our model configuration demonstrates the potential for significant weakening—even shutdown—of the glacial AMOC under a fully glaciated AM. This behaviour contrasts with PMIP-class simulations, in which glacial AMOC is often maintained or strengthened due to enhanced surface salinity and brine rejection (Zhang et al. 2013; Kageyama et al. 2021; Knorr et al. 2021). By explicitly resolving sub-ice cavity circulation, freshwater routing, and pressure-gradient-driven gyres, our approach captures key dynamical processes absent from standard model frameworks.

Together, these results suggest that conventional representations of glacial boundary conditions may systematically underestimate the impact of ice shelf–ocean

interactions on deep overturning circulation. Explicitly resolving sub-ice-shelf dynamics and Arctic gateway geometry appears essential for capturing physically plausible glacial ocean states.

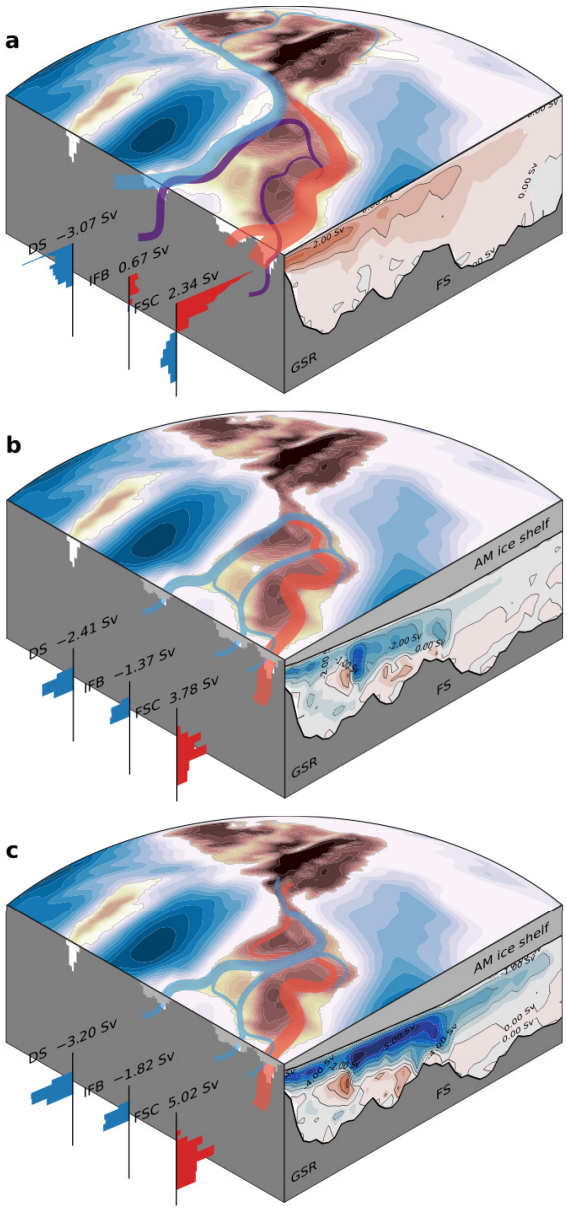


Fig. 1 Ocean circulation in the AM basin. Overturning circulation, gyre sketch and vertical structure of volume flux through GSR channels in (a) CTRL, (b) ICE, and (c) ICEfw. In the gyre sketch, red denotes warm and salty water, blue denotes cold and fresh water, and purple denotes dense water. DS: Denmark Strait; IFB: Iceland–Faroe Branch; FSC: Faroe–Shetland Channel; GSR: Greenland–Scotland Ridge; FS: Fram Strait.

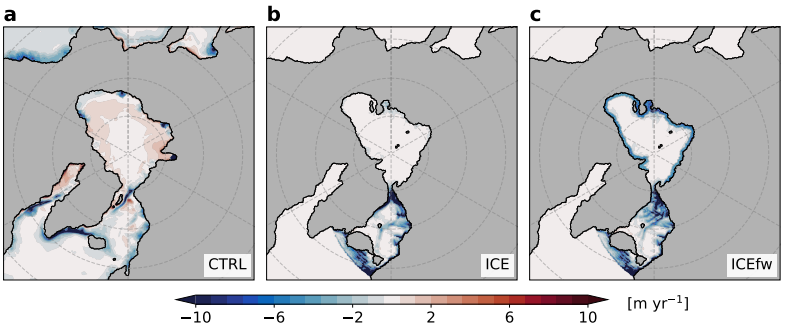


Fig. 2 Freshwater fluxes into the AM basin. Freshwater flux rates from the three simulations, where negative values denote freshwater input to the ocean. (a) CTRL includes contributions from river runoff, atmosphere, and sea ice; (b) ICE includes only ice-shelf basal melt; (c) ICEfw includes basal melt and subglacial freshwater discharge.

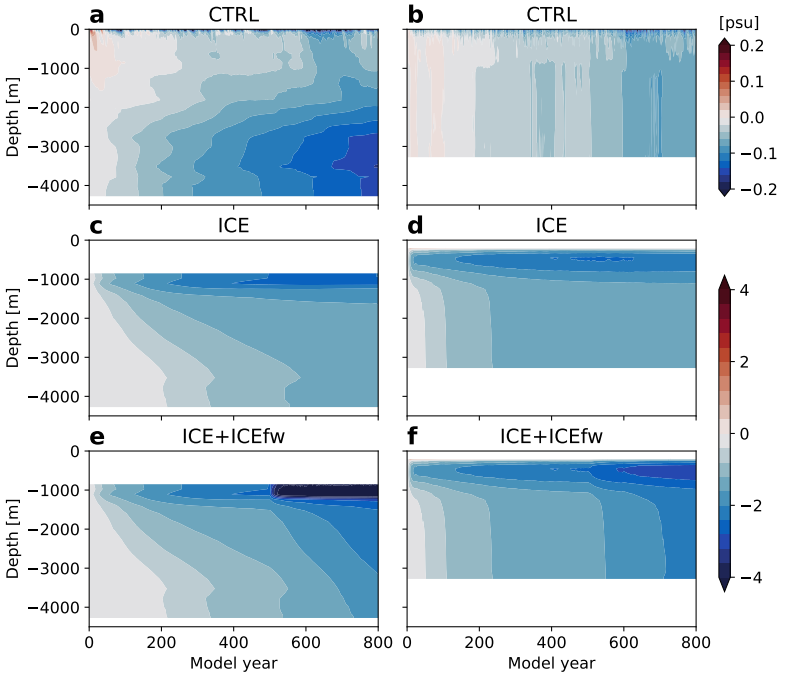


Fig. 3 Time series of AM salinity anomaly. Basin-averaged salinity anomalies relative to initial conditions across vertical layers. Panels (a,c,e) correspond to the Arctic Ocean; panels (b,d,f) to the Nordic Seas. Simulations shown are (a,b) CTRL, (c,d) ICE, and (e,f) ICEfw (with the first 500 years from ICE). Note that color scales vary across panels.

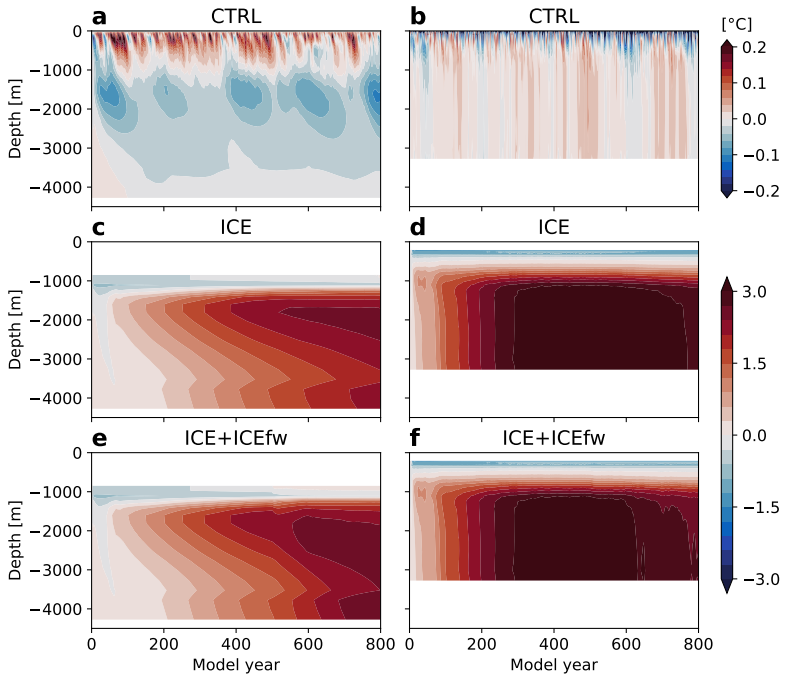


Fig. 4 Time series of AM temperature anomaly. Same as Fig. 3, but for temperature anomalies.

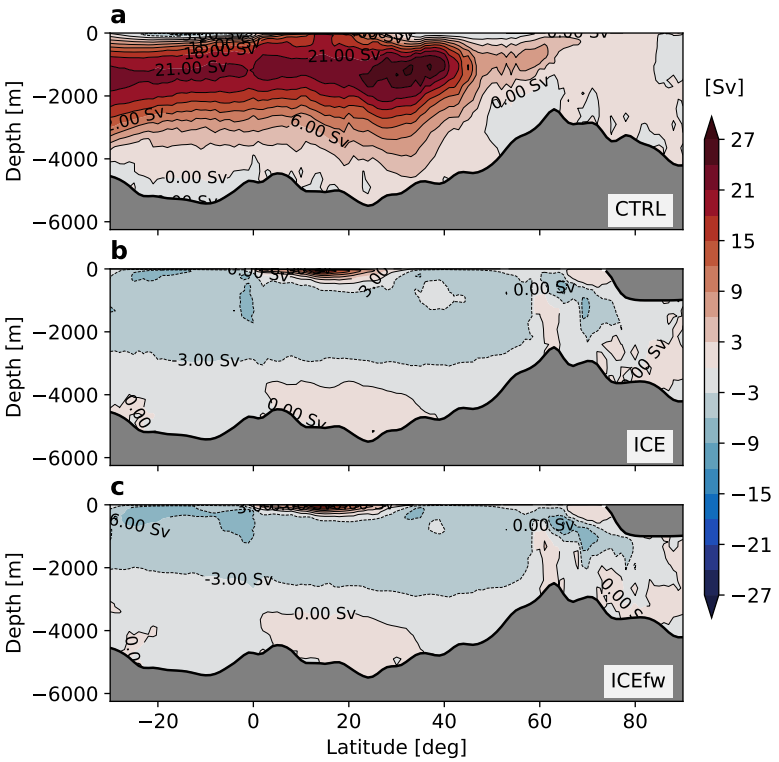


Fig. 5 Atlantic Meridional Overturning Circulation (AMOC). AMOC structure in (a) CTRL, (b) ICE, and (c) ICEfw. Blue and red contours indicate counterclockwise and clockwise overturning cells, respectively.

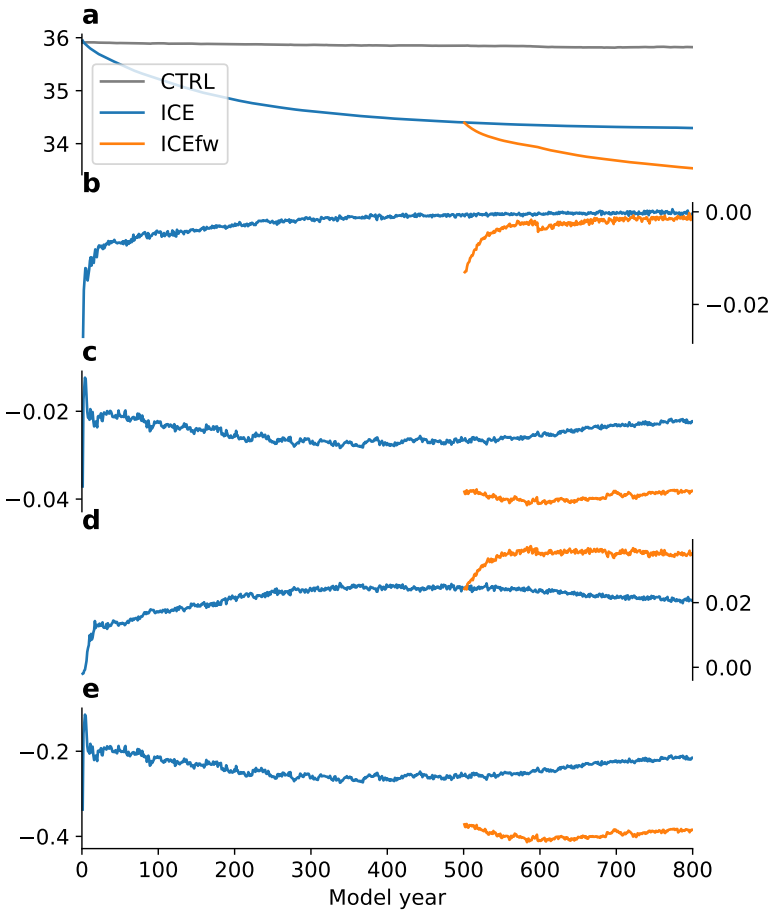


Fig. 6 Diagnosis of AM salinity. Time series of (a) AM-averaged salinity, (b) trend of AM-averaged salinity, (c) trend of AM-averaged salinity attributed to ice-shelf basal melt, (d) trend of AM-averaged salinity attributed to salt flux through GSR channels, (e) ice-shelf basal melt rate within the AM basin (negative for melting). The y-axis unit for panel (a) is psu, for panels (b–d) is psu yr^{-1}, for panel (e) is Sv.

Appendix A Methods

This study employs the Alfred Wegener Institute Earth System Model version 2 (AWI-ESM2), which integrates the ocean–sea ice model FESOM2 (Danilov et al. 2017), the atmospheric model ECHAM6 (Stevens et al. 2013), and the land-surface model JSBACH (Raddatz et al. 2007; Reick et al. 2013). JSBACH features dynamic vegetation and a hydrological discharge module (Hagemann and Dümenil 1997). These components are coupled via the OASIS3-MCT coupler (Valcke 2013). The ice-sheet component is non-interactive; ice sheets are prescribed as static boundary conditions throughout the simulation.

The ocean component, FESOM2, utilises unstructured triangular meshes, which allow improved resolution in critical regions such as the Equator, the poles, and coastal zones. However, mesh elements and nodes do not remain consistent when coastlines change. To manage this, we apply a mesh-cutting strategy so that, despite differing land–sea masks between control and comparison runs, the ocean mesh remains identical within wet regions.

Ice shelf–ocean interaction is represented via an ice-cavity module within FESOM2. This module applies a rigid-lid approximation atop the ocean, complementing the standard z-star vertical coordinate. Interaction at the ice shelf–ocean interface is governed by a three-equation model (Hellmer and Olbers 1989; Holland and Jenkins 1999; Jenkins 1991), which computes freshwater, heat, and momentum fluxes. As with ice sheets, ice shelves are prescribed with fixed grounding lines, thicknesses, and calving fronts. A prior implementation of AWI-ESM2 with cavity dynamics and mesh cutting—focused on Antarctic configurations—can be found in Song et al. (2025).

A.1 The control simulation

We adopt LGM as the climatological background. In the control simulation, CTRL, topography is based on the GLAC-1D reconstruction (Tarasov et al. 2012), and

orbital and greenhouse gas forcings follow the Paleoclimate Modelling Intercomparison Project Phase 4 (PMIP4) protocol (Kageyama et al. 2017). Although extreme glaciation in the Arctic is considered more likely during MIS 4 or 6 than MIS 2 (Jakobsson et al. 2014; Geibert et al. 2021), we simulate LGM (21 ka, MIS 2) instead of the Penultimate Glacial Maximum (PGM, 140 ka, MIS 6), due to the better-constrained ice-sheet reconstruction and the availability of a spun-up LGM state. Given our focus on the climate impact of a kilometre-thick basin-wide ice shelf, differences between LGM and PGM in topography, orbital parameters, and greenhouse gas levels are not central to our investigation.

All simulations are initialised from rest, but with LGM climatology for ocean temperature and salinity, regridded from a prior LGM spin-up exceeding 5000 years (X. Shi, personal communication). We avoid a warm restart to maintain numerical stability, as sudden loading of a kilometre-thick ice shelf would destabilise the ocean velocity field. Because the deep ocean originates from a spun-up state, 800 model years of simulation are deemed sufficient for atmospheric, land, and upper-ocean adjustment.

A.2 Ice-shelf setup

To examine the hypothesis of a kilometre-thick basin-wide ice shelf, we implement a comparison simulation, ICE. Relative to CTRL, ICE includes an idealised ice shelf covering the entire AM basin—comprising the Arctic Ocean, Nordic Seas, and a narrow extension south of the GSR (Fig. A1b). This configuration reflects the maximum extent proposed in earlier studies (Hughes et al. 1977; Jakobsson et al. 2014). We do not consider additional ice shelves outside the AM region (e.g. Baffin Bay).

The prescribed ice-shelf thickness is 1000 m across the Arctic Ocean, gradually decreasing southward from the Fram Strait to the calving front. Thickness values follow earlier ice-sheet–shelf modelling efforts (Nilsson et al. 2017; Gasson et al. 2018).

For simplicity, we ignore back-stress effects on the central Arctic ridge by maintaining uniform thickness, and also idealise the base geometry as linearly sloping.

The ICE ocean mesh is a submesh of CTRL, modified to exclude regions where bathymetry lies above the prescribed ice-shelf base—these shallow shelves are treated as grounded ice and thus removed to maintain valid cavity geometry. Since ice-shelf thickness decreases southward, its value at the calving front governs the AM basin extent and its connectivity to the North Atlantic. Reconstructions do not support complete grounding of ice sheets over the GSR during the Quaternary (Batchelor et al. 2019). Therefore, we tune the ice-shelf thickness at the calving front to preserve all three AM–North Atlantic connecting gateways: the Denmark Strait, the Iceland–Faroe Branch, and the Faroe–Shetland Channel. Accordingly, we set calving-front thickness to 75 m.

Mesh modifications extend to the atmosphere (ECHAM6) and land (JSBACH) components, because the ice shelf affects boundary conditions across all subsystems. The AM ice shelf is treated as a glacier-type surface in the atmosphere, primarily influencing albedo. Cut-off ocean areas are classified as grounded ice. To minimise divergence from CTRL, we retain orography unchanged, keeping the ice shelf's surface altitude at sea level.

In proposing a freshwater-filled Arctic Ocean, Geibert et al. (2021) suggested that seawater was largely displaced by freshwater discharge. While such discharge—including river, lake, and subglacial sources—is spatially uneven (e.g. concentration near East Siberian rivers), we simplify by applying uniform freshwater hosing along the Arctic coast. Here, the Arctic coastline corresponds to the grounding line, and the freshwater is released into the cavity at 1000 m depth using a virtual-salt approach. The discharge rate is 0.1 Sv, close to estimates from CTRL. This simulation, termed ICEfw, is branched from ICE and integrated over 300 model years.

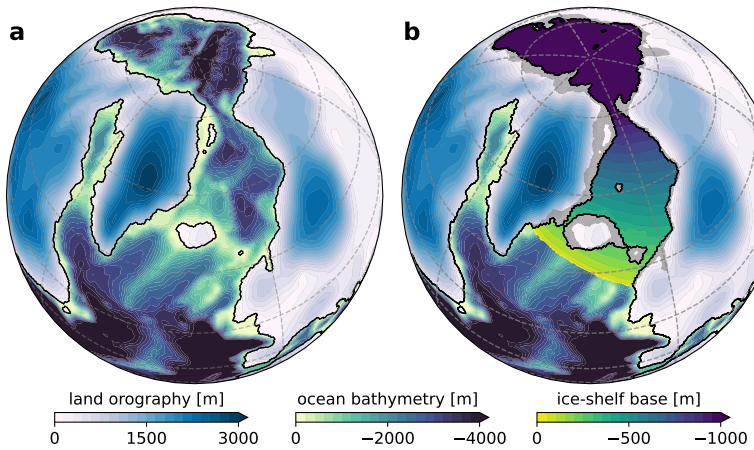


Fig. A1 Model meshes. Mesh configurations for (a) CTRL and (b) ICE/ICEfw. Color maps indicate land elevation, ocean depth, and ice-shelf base. Grey shading in panel (b) denotes areas converted from ocean to grounded ice under the AM ice-shelf setup.

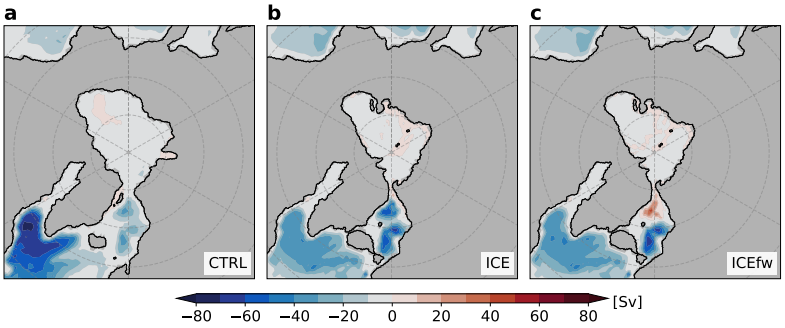


Fig. A2 Barotropic streamfunction. Streamfunction distributions from (a) CTRL, (b) ICE, and (c) ICEfw. Blue contours indicate cyclonic gyres; red contours indicate anticyclonic gyres.

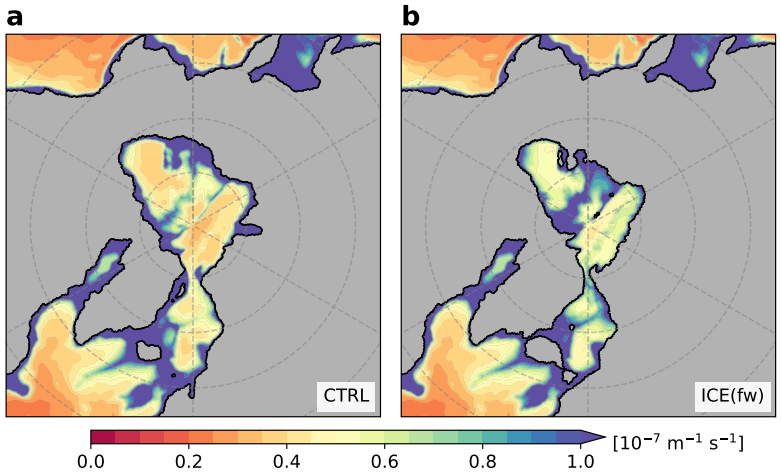


Fig. A3 Contours of f/H. Distributions of planetary vorticity over water thickness (f/H) in (a) CTRL and (b) ICE/ICEfw setups, illustrating topographic control on circulation.

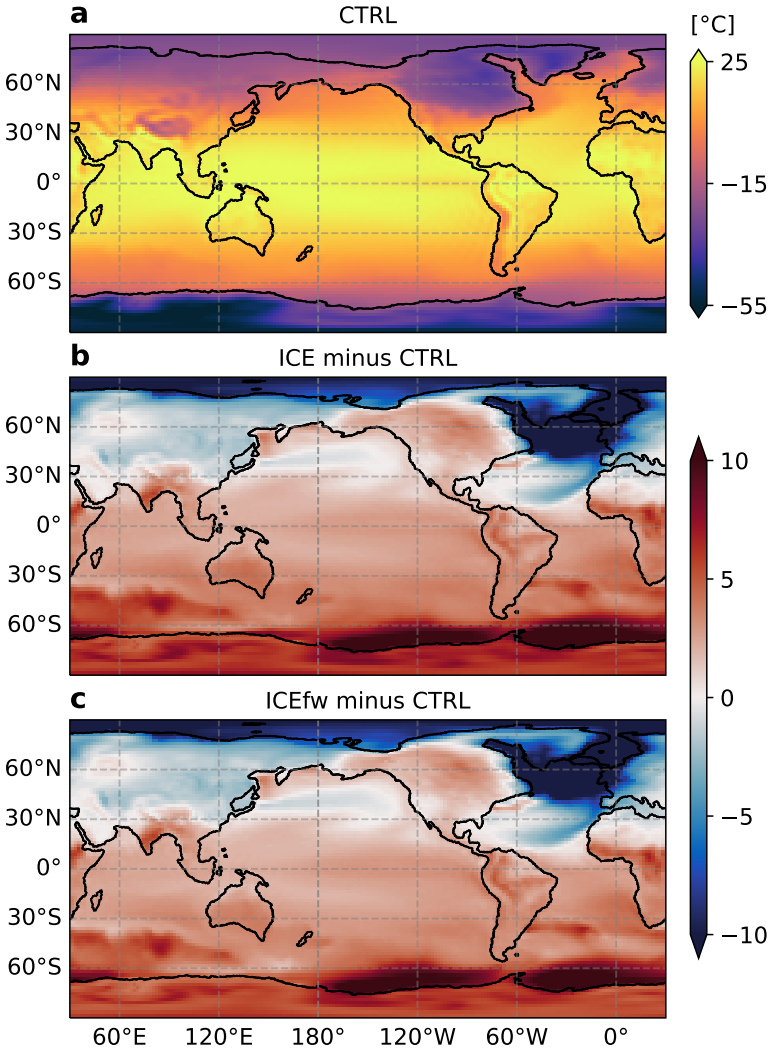


Fig. A4 Surface air temperature. Surface air temperature results from (a) CTRL, (b) ICE and (c) ICEfw. Panels (b) and (c) show deviations from CTRL.

Acknowledgments

The authors acknowledge that generative pre-trained transformer (GPT) tools were employed during manuscript preparation, specifically, grammar checking and polishing the writing. The authors thank Walter Geibert for fruitful discussions and Martin Werner for helping with the model's boundary condition files. PS is funded by the China Scholarship Council (grant no. 201906330073) and the German Federal Ministry of Education and Research (BMBF) funded project PalMod (grant number 01LP2317A to GK and GL). GL and GK are supported by the ERC synergy grant 'i2B' (grant no. 101118519). All experiments have been conducted on Levante, the high-performance computing system at the German Climate Computing Centre.

Author contributions

PS conducted all experiments and completed the first draft. PS, GK and GL contributed to the analysis of the results and the preparation and revision of the manuscript. Correspondence and requests for materials should be addressed to the corresponding author.

Competing interests

The authors declare no competing interests.

Code and data availability

The model source code and its configuration are archived at https://doi.org/10.5281/zenodo.18588686. Model output over the last 100 simulation years and the post-processing routines are archived at https://doi.org/10.5281/zenodo.18588596. The full simulation results are available from the corresponding author upon reasonable request.

References

Adusumilli S, Fricker HA, Medley B, et al (2020) Interannual variations in meltwater input to the Southern Ocean from Antarctic ice shelves. Nature Geoscience 13(9):616–620. https://doi.org/10.1038/s41561-020-0616-z

Batchelor CL, Margold M, Krapp M, et al (2019) The configuration of Northern Hemisphere ice sheets through the Quaternary. Nature Communications 10(1):3713. https://doi.org/10.1038/s41467-019-11601-2

Böhm E, Lippold J, Gutjahr M, et al (2015) Strong and deep Atlantic meridional overturning circulation during the last glacial cycle. Nature 517(7532):73–76. https://doi.org/10.1038/nature14059, URL https://www.nature.com/articles/nature14059

Broecker WS (1975) Floating Glacial Ice Caps in the Arctic Ocean. Science 188(4193):1116–1118. https://doi.org/10.1126/science.188.4193.1116

Colleoni F, Krinner G, Jakobsson M (2010) The role of an Arctic ice shelf in the climate of the MIS 6 glacial maximum (140 ka). Quaternary Science Reviews 29(25-26):3590–3597. https://doi.org/10.1016/j.quascirev.2010.06.023

Colleoni F, Liakka J, Krinner G, et al (2011) The sensitivity of the Late Saalian (140 ka) and LGM (21 ka) Eurasian ice sheets to sea surface conditions. Climate Dynamics 37(3-4):531–553. https://doi.org/10.1007/s00382-010-0870-7

Cronin TM, Dwyer GS, Farmer J, et al (2012) Deep Arctic Ocean warming during the last glacial cycle. Nature Geoscience 5(9):631–634. https://doi.org/10.1038/ngeo1557

Danilov S, Sidorenko D, Wang Q, et al (2017) The finite-volume sea ice-Ocean model (FESOM2). Geoscientific Model Development 10(2):765–789. https://doi.org/10.

5194/gmd-10-765-2017

Dowdeswell J, Jakobsson M, Hogan K, et al (2010) High-resolution geophysical observations of the Yermak Plateau and northern Svalbard margin: implications for ice-sheet grounding and deep-keeled icebergs. Quaternary Science Reviews 29(25-26):3518–3531. https://doi.org/10.1016/j.quascirev.2010.06.002, URL http://dx.doi.org/10.1016/j.quascirev.2010.06.002https://linkinghub.elsevier.com/retrieve/pii/S0277379110001940

Dowdeswell JA, Ottesen D (2024) Iceberg ploughmarks and glacial lineations on Jan Mayen Ridge: Evidence for past iceberg and possible ice-shelf grounding in deep water. Quaternary Science Reviews 338(July):108838. https://doi.org/10.1016/j.quascirev.2024.108838, URL https://doi.org/10.1016/j.quascirev.2024.108838https://linkinghub.elsevier.com/retrieve/pii/S0277379124003391

Engels JL, Edwards MH, Polyak L, et al (2008) Seafloor evidence for ice shelf flow across the Alaska–Beaufort margin of the Arctic Ocean. Earth Surface Processes and Landforms 33(7):1047–1063. https://doi.org/10.1002/esp.1601

Gasson EGW, DeConto RM, Pollard D, et al (2018) Numerical simulations of a kilometre-thick Arctic ice shelf consistent with ice grounding observations. Nature Communications 9(1):1510. https://doi.org/10.1038/s41467-018-03707-w

Geibert W, Matthiessen J, Stimac I, et al (2021) Glacial episodes of a freshwater Arctic Ocean covered by a thick ice shelf. Nature 590(7844):97–102. https://doi.org/10.1038/s41586-021-03186-y

Griffiths SD, Peltier WR (2008) Megatides in the Arctic Ocean under glacial conditions. Geophysical Research Letters 35(8):L08605. https://doi.org/10.1029/2008GL033263

Grosfeld K, Gerdes R, Determann J (1997) Thermohaline circulation and interaction between ice shelf cavities and the adjacent open ocean. Journal of Geophysical Research: Oceans 102(C7):15595–15610. https://doi.org/10.1029/97JC00891, URL https://agupubs.onlinelibrary.wiley.com/doi/10.1029/97JC00891

Hagemann S, Dümenil L (1997) A parametrization of the lateral waterflow for the global scale. Climate Dynamics 14(1):17–31. https://doi.org/10.1007/s003820050205

Hellmer HH, Olbers D (1989) A two-dimensional model for the thermohaline circulation under an ice shelf. Antarctic Science 1(4):325–336. https://doi.org/10.1017/S0954102089000490

Hillaire-Marcel C, Myers PG, Marshall S, et al (2022) Challenging the hypothesis of an Arctic Ocean lake during recent glacial episodes. Journal of Quaternary Science 37(4):559–567. https://doi.org/10.1002/jqs.3421

Holland DM, Jenkins A (1999) Modeling Thermodynamic Ice–Ocean Interactions at the Base of an Ice Shelf. Journal of Physical Oceanography 29(8):1787–1800. https://doi.org/10.1175/1520-0485(1999)029⟨1787:MTIOIA⟩2.0.CO;2

Hughes T, Denton GH, Grosswald MG (1977) Was there a late-Würm Arctic Ice Sheet? Nature 266(5603):596–602. https://doi.org/10.1038/266596a0

Jakobsson M, Backman J, Rudels B, et al (2007) The early Miocene onset of a ventilated circulation regime in the Arctic Ocean. Nature 447(7147):986–990. https://doi.org/10.1038/nature05924

Jakobsson M, Polyak L, Edwards M, et al (2008) Glacial geomorphology of the Central Arctic Ocean: the Chukchi Borderland and the Lomonosov Ridge. Earth Surface Processes and Landforms 33(4):526–545. https://doi.org/10.1002/esp.1667

Jakobsson M, Nilsson J, O'Regan M, et al (2010) An Arctic Ocean ice shelf during MIS 6 constrained by new geophysical and geological data. Quaternary Science Reviews 29(25-26):3505–3517. https://doi.org/10.1016/j.quascirev.2010.03.015

Jakobsson M, Andreassen K, Bjarnadóttir LR, et al (2014) Arctic Ocean glacial history. Quaternary Science Reviews 92:40–67. https://doi.org/10.1016/j.quascirev.2013.07.033

Jakobsson M, Nilsson J, Anderson L, et al (2016) Evidence for an ice shelf covering the central Arctic Ocean during the penultimate glaciation. Nature Communications 7(1):10365. https://doi.org/10.1038/ncomms10365

Jang K, Woo KS, Kim JK, et al (2023) Arctic deep-water anoxia and its potential role for ocean carbon sink during glacial periods. Communications Earth & Environment 4(1):45. https://doi.org/10.1038/s43247-023-00708-6

Jenkins A (1991) A one-dimensional model of ice shelf-ocean interaction. Journal of Geophysical Research 96(C11):20671. https://doi.org/10.1029/91JC01842

Kageyama M, Albani S, Braconnot P, et al (2017) The PMIP4 contribution to CMIP6 – Part 4: Scientific objectives and experimental design of the PMIP4-CMIP6 Last Glacial Maximum experiments and PMIP4 sensitivity experiments. Geoscientific Model Development 10(11):4035–4055. https://doi.org/10.5194/gmd-10-4035-2017

Kageyama M, Harrison SP, Kapsch ML, et al (2021) The PMIP4 Last Glacial Maximum experiments: preliminary results and comparison with the PMIP3 simulations. Climate of the Past 17(3):1065–1089. https://doi.org/10.5194/cp-17-1065-2021, URL https://cp.copernicus.org/articles/17/1065/2021/

Knies J, Smik L, Song P, et al (2025) Seasonal sea ice characterized the glacial Arctic-Atlantic gateway over the past 750,000 years. Science Advances 11(27):1–8. https://doi.org/10.1126/sciadv.adu7681, URL https://www.science.org/doi/10.1126/sciadv.adu7681

Knorr G, Barker S, Zhang X, et al (2021) A salty deep ocean as a prerequisite for glacial termination. Nature Geoscience 14(12):930–936. https://doi.org/10.1038/s41561-021-00857-3, URL https://www.nature.com/articles/s41561-021-00857-3

Knutti R, Flückiger J, Stocker TF, et al (2004) Strong hemispheric coupling of glacial climate through freshwater discharge and ocean circulation. Nature 430(7002):851–856. https://doi.org/10.1038/nature02786, URL https://www.nature.com/articles/nature02786

Lewis EL, Perkin RG (1986) Ice pumps and their rates. Journal of Geophysical Research: Oceans 91(C10):11756–11762. https://doi.org/10.1029/JC091iC10p11756, URL https://agupubs.onlinelibrary.wiley.com/doi/10.1029/JC091iC10p11756

Losch M (2008) Modeling ice shelf cavities in a z coordinate ocean general circulation model. Journal of Geophysical Research 113(C8):C08043. https://doi.org/10.1029/2007JC004368

Mathiot P, Jenkins A, Harris C, et al (2017) Explicit representation and parametrised impacts of under ice shelf seas in the z* coordinate ocean model NEMO 3.6. Geoscientific Model Development 10(7):2849–2874. https://doi.org/10.5194/gmd-10-2849-2017

Mercer J (1970) A former ice sheet in the Arctic Ocean? Palaeogeography, Palaeoclimatology, Palaeoecology 8(1):19–27. https://doi.org/10.1016/0031-0182(70)90076-3

Niessen F, Hong JK, Hegewald A, et al (2013) Repeated Pleistocene glaciation of the East Siberian continental margin. Nature Geoscience 6(10):842–846. https://doi.org/10.1038/ngeo1904

Nilsson J, Jakobsson M, Borstad C, et al (2017) Ice-shelf damming in the glacial Arctic Ocean: dynamical regimes of a basin-covering kilometre-thick ice shelf. The Cryosphere 11(4):1745–1765. https://doi.org/10.5194/tc-11-1745-2017

Nilsson J, van Dongen E, Jakobsson M, et al (2023) Hydraulic suppression of basal glacier melt in sill fjords. The Cryosphere 17(6):2455–2476. https://doi.org/10.5194/tc-17-2455-2023

Polyak L, Edwards MH, Coakley BJ, et al (2001) Ice shelves in the Pleistocene Arctic Ocean inferred from glaciogenic deep-sea bedforms. Nature 410(6827):453–457. https://doi.org/10.1038/35068536

Polyak L, Darby DA, Bischof JF, et al (2007) Stratigraphic constraints on late Pleistocene glacial erosion and deglaciation of the Chukchi margin, Arctic Ocean. Quaternary Research 67(2):234–245. https://doi.org/10.1016/j.yqres.2006.08.001

Raddatz TJ, Reick CH, Knorr W, et al (2007) Will the tropical land biosphere dominate the climate–carbon cycle feedback during the twenty-first century? Climate Dynamics 29(6):565–574. https://doi.org/10.1007/s00382-007-0247-8

Rahmstorf S (2002) Ocean circulation and climate during the past 120,000 years. Nature 419(6903):207–214. https://doi.org/10.1038/nature01090, URL https://www.nature.com/articles/nature01090

Reick CH, Raddatz T, Brovkin V, et al (2013) Representation of natural and anthropogenic land cover change in MPI-ESM. Journal of Advances in Modeling Earth Systems 5(3):459–482. https://doi.org/10.1002/jame.20022

Song P, Scholz P, Knorr G, et al (2025) Regional conditions determine thresholds of accelerated Antarctic basal melt in climate projection. Nature Climate Change 15(5):521–527. https://doi.org/10.1038/s41558-025-02306-0, URL https://www.nature.com/articles/s41558-025-02306-0

Spielhagen RF, Scholten JC, Bauch HA, et al (2022) No freshwater-filled glacial Arctic Ocean. Nature 602(7895):E1–E3. https://doi.org/10.1038/s41586-021-04089-8

Stärz M, Jokat W, Knorr G, et al (2017) Threshold in North Atlantic-Arctic Ocean circulation controlled by the subsidence of the Greenland-Scotland Ridge. Nature Communications 8(1):15681. https://doi.org/10.1038/ncomms15681, URL https://www.nature.com/articles/ncomms15681

Stein R, Fahl K, Gierz P, et al (2017) Arctic Ocean sea ice cover during the penultimate glacial and the last interglacial. Nature Communications 8(1):373. https://doi.org/10.1038/s41467-017-00552-1

Stern AA, Holland DM, Holland PR, et al (2014) The effect of geometry on ice shelf ocean cavity ventilation: a laboratory experiment. Experiments in Fluids 55(5):1719. https://doi.org/10.1007/s00348-014-1719-3, URL http://link.springer.com/10.1007/s00348-014-1719-3

Stevens B, Giorgetta M, Esch M, et al (2013) Atmospheric component of the MPI-M Earth System Model: ECHAM6. Journal of Advances in Modeling Earth Systems 5(2):146–172. https://doi.org/10.1002/jame.20015

Tarasov L, Dyke AS, Neal RM, et al (2012) A data-calibrated distribution of deglacial chronologies for the North American ice complex from glaciological modeling. Earth and Planetary Science Letters 315-316:30–40. https://doi.org/10.1016/j.epsl.2011.09.010

Thornalley DJR, Bauch HA, Gebbie G, et al (2015) A warm and poorly ventilated deep Arctic Mediterranean during the last glacial period. Science 349(6249):706–710. https://doi.org/10.1126/science.aaa9554

Timmermans ML, Garrett C, Carmack E (2003) The thermohaline structure and evolution of the deep waters in the Canada Basin, Arctic Ocean. Deep Sea Research Part I: Oceanographic Research Papers 50(10-11):1305–1321. https://doi.org/10.1016/S0967-0637(03)00125-0, URL https://linkinghub.elsevier.com/retrieve/pii/S0967063703001250

Valcke S (2013) The OASIS3 coupler: a European climate modelling community software. Geoscientific Model Development 6(2):373–388. https://doi.org/10.5194/gmd-6-373-2013

Zhang X, Lohmann G, Knorr G, et al (2013) Different ocean states and transient characteristics in Last Glacial Maximum simulations and implications for deglaciation. Climate of the Past 9(5):2319–2333. https://doi.org/10.5194/cp-9-2319-2013, URL https://cp.copernicus.org/articles/9/2319/2013/